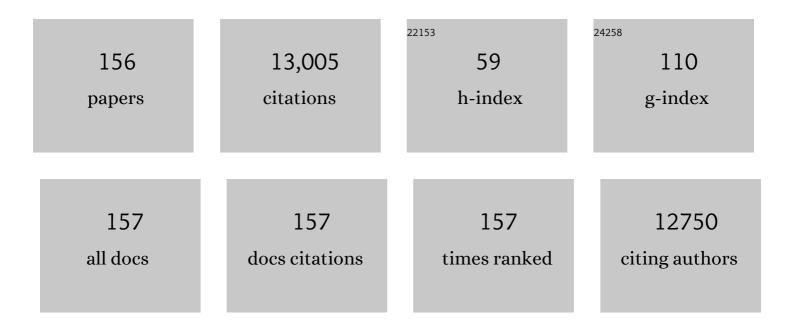
## **Patrick Hostert**

List of Publications by Year in descending order

Source: https://exaly.com/author-pdf/5138802/publications.pdf Version: 2024-02-01



#	Article	IF	CITATIONS
1	Current status of Landsat program, science, and applications. Remote Sensing of Environment, 2019, 225, 127-147.	11.0	586
2	The EnMAP Spaceborne Imaging Spectroscopy Mission for Earth Observation. Remote Sensing, 2015, 7, 8830-8857.	4.0	529
3	A Review of the Application of Optical and Radar Remote Sensing Data Fusion to Land Use Mapping and Monitoring. Remote Sensing, 2016, 8, 70.	4.0	459
4	Mapping farmland abandonment and recultivation across Europe using MODIS NDVI time series. Remote Sensing of Environment, 2015, 163, 312-325.	11.0	392
5	Land system science and sustainable development of the earth system: A global land project perspective. Anthropocene, 2015, 12, 29-41.	3.3	388
6	Patterns and drivers of post-socialist farmland abandonment in Western Ukraine. Land Use Policy, 2011, 28, 552-562.	5.6	369
7	Intra-annual reflectance composites from Sentinel-2 and Landsat for national-scale crop and land cover mapping. Remote Sensing of Environment, 2019, 220, 135-151.	11.0	307
8	Benefits of the free and open Landsat data policy. Remote Sensing of Environment, 2019, 224, 382-385.	11.0	291
9	Bringing an ecological view of change to Landsatâ€based remote sensing. Frontiers in Ecology and the Environment, 2014, 12, 339-346.	4.0	285
10	Challenges and opportunities in mapping land use intensity globally. Current Opinion in Environmental Sustainability, 2013, 5, 484-493.	6.3	279
11	Sensitivity of Support Vector Machines to Random Feature Selection in Classification of Hyperspectral Data. IEEE Transactions on Geoscience and Remote Sensing, 2010, 48, 2880-2889.	6.3	263
12	Cross-border Comparison of Post-socialist Farmland Abandonment in the Carpathians. Ecosystems, 2008, 11, 614-628.	3.4	253
13	Remote sensing of sunâ€induced fluorescence to improve modeling of diurnal courses of gross primary production (GPP). Global Change Biology, 2010, 16, 171-186.	9.5	246
14	Forest disturbances, forest recovery, and changes in forest types across the Carpathian ecoregion from 1985 to 2010 based on Landsat image composites. Remote Sensing of Environment, 2014, 151, 72-88.	11.0	231
15	A Pixel-Based Landsat Compositing Algorithm for Large Area Land Cover Mapping. IEEE Journal of Selected Topics in Applied Earth Observations and Remote Sensing, 2013, 6, 2088-2101.	4.9	226
16	Land cover mapping of large areas using chain classification of neighboring Landsat satellite images. Remote Sensing of Environment, 2009, 113, 957-964.	11.0	201
17	Mapping the extent of abandoned farmland in Central and Eastern Europe using MODIS time series satellite data. Environmental Research Letters, 2013, 8, 035035.	5.2	197
18	Mapping megacity growth with multi-sensor data. Remote Sensing of Environment, 2010, 114, 426-439.	11.0	190

#	Article	IF	CITATIONS
19	Urban vegetation classification: Benefits of multitemporal RapidEye satellite data. Remote Sensing of Environment, 2013, 136, 66-75.	11.0	189
20	The EnMAP-Box—A Toolbox and Application Programming Interface for EnMAP Data Processing. Remote Sensing, 2015, 7, 11249-11266.	4.0	185
21	Forest cover change and illegal logging in the Ukrainian Carpathians in the transition period from 1988 to 2007. Remote Sensing of Environment, 2009, 113, 1194-1207.	11.0	182
22	Canopy mortality has doubled in Europe's temperate forests over the last three decades. Nature Communications, 2018, 9, 4978.	12.8	182
23	Land use and land cover change in Inner Mongolia - understanding the effects of China's re-vegetation programs. Remote Sensing of Environment, 2018, 204, 918-930.	11.0	165
24	Forest Stand Species Mapping Using the Sentinel-2 Time Series. Remote Sensing, 2019, 11, 1197.	4.0	162
25	Post-Soviet farmland abandonment, forest recovery, and carbon sequestration in western Ukraine. Global Change Biology, 2011, 17, 1335-1349.	9.5	159
26	Ten facts about land systems for sustainability. Proceedings of the National Academy of Sciences of the United States of America, 2022, 119, .	7.1	157
27	Mining dense Landsat time series for separating cropland and pasture in a heterogeneous Brazilian savanna landscape. Remote Sensing of Environment, 2015, 156, 490-499.	11.0	151
28	Cross-border comparison of land cover and landscape pattern in Eastern Europe using a hybrid classification technique. Remote Sensing of Environment, 2006, 103, 449-464.	11.0	149
29	Carbon emissions from agricultural expansion and intensification in the Chaco. Global Change Biology, 2017, 23, 1902-1916.	9.5	142
30	Agricultural land change in the Carpathian ecoregion after the breakdown of socialism and expansion of the European Union. Environmental Research Letters, 2013, 8, 045024.	5.2	139
31	Mapping land cover in complex Mediterranean landscapes using Landsat: Improved classification accuracies from integrating multi-seasonal and synthetic imagery. Remote Sensing of Environment, 2015, 156, 527-536.	11.0	135
32	Remote sensing of forest insect disturbances: Current state and future directions. International Journal of Applied Earth Observation and Geoinformation, 2017, 60, 49-60.	2.8	134
33	Mapping pan-European land cover using Landsat spectral-temporal metrics and the European LUCAS survey. Remote Sensing of Environment, 2019, 221, 583-595.	11.0	134
34	From teleconnection to telecoupling: taking stock of an emerging framework in land system science. Journal of Land Use Science, 2016, 11, 131-153.	2.2	132
35	Forest restitution and protected area effectiveness in post-socialist Romania. Biological Conservation, 2012, 146, 204-212.	4.1	126
36	Coupling spectral unmixing and trend analysis for monitoring of long-term vegetation dynamics in Mediterranean rangelands. Remote Sensing of Environment, 2003, 87, 183-197.	11.0	123

#	Article	IF	CITATIONS
37	POST-SOCIALIST FOREST DISTURBANCE IN THE CARPATHIAN BORDER REGION OF POLAND, SLOVAKIA, AND UKRAINE. , 2007, 17, 1279-1295.		121
38	Support vector regression and synthetically mixed training data for quantifying urban land cover. Remote Sensing of Environment, 2013, 137, 184-197.	11.0	120
39	Mapping the timing of cropland abandonment and recultivation in northern Kazakhstan using annual Landsat time series. Remote Sensing of Environment, 2018, 213, 49-60.	11.0	114
40	AROSICS: An Automated and Robust Open-Source Image Co-Registration Software for Multi-Sensor Satellite Data. Remote Sensing, 2017, 9, 676.	4.0	113
41	Rapid land use change after socio-economic disturbances: the collapse of the Soviet Union versus Chernobyl. Environmental Research Letters, 2011, 6, 045201.	5.2	112
42	Using annual time-series of Landsat images to assess the effects of forest restitution in post-socialist Romania. Remote Sensing of Environment, 2012, 118, 199-214.	11.0	112
43	Mapping cropland-use intensity across Europe using MODIS NDVI time series. Environmental Research Letters, 2016, 11, 024015.	5.2	107
44	Characterizing spectral–temporal patterns of defoliator and bark beetle disturbances using Landsat time series. Remote Sensing of Environment, 2015, 170, 166-177.	11.0	104
45	European Bison habitat in the Carpathian Mountains. Biological Conservation, 2010, 143, 908-916.	4.1	101
46	Mapping Rubber Plantations and Natural Forests in Xishuangbanna (Southwest China) Using Multi-Spectral Phenological Metrics from MODIS Time Series. Remote Sensing, 2013, 5, 2795-2812.	4.0	97
47	Mapping of crop types and crop sequences with combined time series of Sentinel-1, Sentinel-2 and Landsat 8 data for Germany. Remote Sensing of Environment, 2022, 269, 112831.	11.0	95
48	Monitoring coniferous forest biomass change using a Landsat trajectory-based approach. Remote Sensing of Environment, 2013, 139, 277-290.	11.0	94
49	National-scale mapping of building height using Sentinel-1 and Sentinel-2 time series. Remote Sensing of Environment, 2021, 252, 112128.	11.0	93
50	Cross-border forest disturbance and the role of natural rubber in mainland Southeast Asia using annual Landsat time series. Remote Sensing of Environment, 2015, 169, 438-453.	11.0	87
51	How Normalized Difference Vegetation Index (NDVI) Trendsfrom Advanced Very High Resolution Radiometer (AVHRR) and SystA¨me Probatoire d'Observation de la Terre VEGETATION (SPOT VGT) Time Series Differ in Agricultural Areas: An Inner Mongolian Case Study. Remote Sensing, 2012, 4, 3364-3389.	4.0	84
52	Towards national-scale characterization of grassland use intensity from integrated Sentinel-2 and Landsat time series. Remote Sensing of Environment, 2020, 238, 111124.	11.0	83
53	Differences in Landsat-based trend analyses in drylands due to the choice of vegetation estimate. Remote Sensing of Environment, 2011, 115, 1408-1420.	11.0	80
54	imageRF – A user-oriented implementation for remote sensing image analysis with Random Forests. Environmental Modelling and Software, 2012, 35, 192-193.	4.5	79

#	Article	IF	CITATIONS
55	The forgotten D: challenges of addressing forest degradation in complex mosaic landscapes under REDD+. Geografisk Tidsskrift, 2012, 112, 63-76.	0.6	76
56	Mapping Brazilian savanna vegetation gradients with Landsat time series. International Journal of Applied Earth Observation and Geoinformation, 2016, 52, 361-370.	2.8	71
57	Mental health in the slums of Dhaka - a geoepidemiological study. BMC Public Health, 2012, 12, 177.	2.9	68
58	Continued loss of temperate old-growth forests in the Romanian Carpathians despite an increasing protected area network. Environmental Conservation, 2013, 40, 182-193.	1.3	68
59	Unravelling the link between global rubber price and tropical deforestation in Cambodia. Nature Plants, 2019, 5, 47-53.	9.3	65
60	Using Landsat time series for characterizing forest disturbance dynamics in the coupled human and natural systems of Central Europe. ISPRS Journal of Photogrammetry and Remote Sensing, 2017, 130, 453-463.	11.1	64
61	Extending the vegetation–impervious–soil model using simulated EnMAP data and machine learning. Remote Sensing of Environment, 2015, 158, 69-80.	11.0	62
62	Mapping temperate forest tree species using dense Sentinel-2 time series. Remote Sensing of Environment, 2021, 267, 112743.	11.0	61
63	Landsat-based mapping of post-Soviet land-use change to assess the effectiveness of the Oksky and Mordovsky protected areas in European Russia. Remote Sensing of Environment, 2013, 133, 38-51.	11.0	58
64	Estimating Fractional Shrub Cover Using Simulated EnMAP Data: A Comparison of Three Machine Learning Regression Techniques. Remote Sensing, 2014, 6, 3427-3445.	4.0	58
65	High-Resolution Maps of Material Stocks in Buildings and Infrastructures in Austria and Germany. Environmental Science & Technology, 2021, 55, 3368-3379.	10.0	57
66	Changes in the spatial patterns of human appropriation of net primary production (HANPP) in Europe 1990–2006. Regional Environmental Change, 2016, 16, 1225-1238.	2.9	55
67	Integrated methodology to assess windthrow impacts on forest stands under climate change. Forest Ecology and Management, 2011, 261, 1799-1810.	3.2	52
68	Evaluating the Remote Sensing and Inventory-Based Estimation of Biomass in the Western Carpathians. Remote Sensing, 2011, 3, 1427-1446.	4.0	52
69	Global Change Research in the Carpathian Mountain Region. Mountain Research and Development, 2009, 29, 282-288.	1.0	51
70	Mapping patterns of urban development in Ouagadougou, Burkina Faso, using machine learning regression modeling with bi-seasonal Landsat time series. Remote Sensing of Environment, 2018, 210, 217-228.	11.0	51
71	Is there a forest transition outside forests? Trajectories of farm trees and effects on ecosystem services in an agricultural landscape in Eastern Germany. Land Use Policy, 2012, 29, 233-243.	5.6	49
72	Mapping grassland mowing events across Germany based on combined Sentinel-2 and Landsat 8 time series. Remote Sensing of Environment, 2022, 269, 112795.	11.0	49

#	Article	IF	CITATIONS
73	Mapping urban-rural gradients of settlements and vegetation at national scale using Sentinel-2 spectral-temporal metrics and regression-based unmixing with synthetic training data. Remote Sensing of Environment, 2020, 246, 111810.	11.0	48
74	Advantages using the thermal infrared (TIR) to detect and quantify semi-arid soil properties. Remote Sensing of Environment, 2015, 163, 296-311.	11.0	47
75	Ensemble Learning From Synthetically Mixed Training Data for Quantifying Urban Land Cover With Support Vector Regression. IEEE Journal of Selected Topics in Applied Earth Observations and Remote Sensing, 2017, 10, 1640-1650.	4.9	47
76	Land use intensity trajectories on Amazonian pastures derived from Landsat time series. International Journal of Applied Earth Observation and Geoinformation, 2015, 41, 1-10.	2.8	46
77	Remote sensing and geospatial technologies in support of a normative land system science: status and prospects. Current Opinion in Environmental Sustainability, 2019, 38, 44-52.	6.3	45
78	Mapping Cropping Practices on a National Scale Using Intra-Annual Landsat Time Series Binning. Remote Sensing, 2019, 11, 232.	4.0	45
79	Annual Landsat time series reveal post-Soviet changes in grazing pressure. Remote Sensing of Environment, 2020, 239, 111667.	11.0	45
80	Correcting brightness gradients in hyperspectral data from urban areas. Remote Sensing of Environment, 2006, 101, 25-37.	11.0	44
81	Using fragmentation to assess degradation of forest edges in Democratic Republic of Congo. Carbon Balance and Management, 2016, 11, 11.	3.2	43
82	How pollution legacies and land use histories shape post-communist forest cover trends in the Western Carpathians. Forest Ecology and Management, 2009, 258, 60-70.	3.2	42
83	Long-term deforestation dynamics in the Brazilian Amazon—Uncovering historic frontier development along the Cuiabá–Santarém highway. International Journal of Applied Earth Observation and Geoinformation, 2016, 44, 61-69.	2.8	41
84	Using Intra-Annual Landsat Time Series for Attributing Forest Disturbance Agents in Central Europe. Forests, 2017, 8, 251.	2.1	41
85	Habitat and population modelling of roe deer using an interactive geographic information system. Ecological Modelling, 1999, 114, 287-304.	2.5	40
86	A highâ€resolution approach to estimating ecosystem respiration at continental scales using operational satellite data. Global Change Biology, 2014, 20, 1191-1210.	9.5	40
87	Mapping the Slums of Dhaka from 2006 to 2010. Dataset Papers in Science, 2014, 2014, 1-7.	1.0	40
88	A spatial epidemiological analysis of self-rated mental health in the slums of Dhaka. International Journal of Health Geographics, 2011, 10, 36.	2.5	38
89	Mapping Annual Land Use and Land Cover Changes Using MODIS Time Series. IEEE Journal of Selected Topics in Applied Earth Observations and Remote Sensing, 2014, 7, 3421-3427.	4.9	38
90	Characterizing 32†years of shrub cover dynamics in southern Portugal using annual Landsat composites and machine learning regression modeling. Remote Sensing of Environment, 2018, 219, 353-364.	11.0	38

#	Article	IF	CITATIONS
91	Characterizing spring phenology of temperate broadleaf forests using Landsat and Sentinel-2 time series. International Journal of Applied Earth Observation and Geoinformation, 2020, 92, 102172.	2.8	38
92	Mapping pasture management in the Brazilian Amazon from dense Landsat time series. Remote Sensing of Environment, 2018, 205, 453-468.	11.0	37
93	Detailed agricultural land classification in the Brazilian cerrado based on phenological information from dense satellite image time series. International Journal of Applied Earth Observation and Geoinformation, 2019, 82, 101872.	2.8	37
94	Modelling avian biodiversity using raw, unclassified satellite imagery. Philosophical Transactions of the Royal Society B: Biological Sciences, 2014, 369, 20130197.	4.0	35
95	Mapping Clearances in Tropical Dry Forests Using Breakpoints, Trend, and Seasonal Components from MODIS Time Series: Does Forest Type Matter?. Remote Sensing, 2016, 8, 657.	4.0	33
96	Generalizing machine learning regression models using multi-site spectral libraries for mapping vegetation-impervious-soil fractions across multiple cities. Remote Sensing of Environment, 2018, 216, 482-496.	11.0	31
97	A Comparison of Advanced Regression Algorithms for Quantifying Urban Land Cover. Remote Sensing, 2014, 6, 6324-6346.	4.0	30
98	Gridded population mapping for Germany based on building density, height and type from Earth Observation data using census disaggregation and bottom-up estimates. PLoS ONE, 2021, 16, e0249044.	2.5	29
99	Mapping Crop Types and Cropping Systems in Nigeria with Sentinel-2 Imagery. Remote Sensing, 2021, 13, 3523.	4.0	29
100	Consequences of nuclear accidents for biodiversity and ecosystem services. Conservation Letters, 2012, 5, 81-89.	5.7	28
101	Livestock Subsidies and Rangeland Degradation in Central Crete. Ecology and Society, 2009, 14, .	2.3	27
102	Reconstructing long term annual deforestation dynamics in ParÃ; and Mato Grosso using the Landsat archive. Remote Sensing of Environment, 2018, 216, 497-513.	11.0	27
103	Post-Soviet Land-Use Change Affected Fire Regimes on the Eurasian Steppes. Ecosystems, 2020, 23, 943-956.	3.4	26
104	Monitoring Natural Ecosystem and Ecological Gradients: Perspectives with EnMAP. Remote Sensing, 2015, 7, 13098-13119.	4.0	25
105	A multi-scale analysis of western spruce budworm outbreak dynamics. Landscape Ecology, 2017, 32, 501-514.	4.2	25
106	Quantifying drought effects in Central European grasslands through regression-based unmixing of intra-annual Sentinel-2 time series. Remote Sensing of Environment, 2022, 268, 112781.	11.0	25
107	Disentangling fractional vegetation cover: Regression-based unmixing of simulated spaceborne imaging spectroscopy data. Remote Sensing of Environment, 2020, 246, 111856.	11.0	22
108	From sample to pixel: multiâ€scale remote sensing data for upscaling aboveground carbon data in heterogeneous landscapes. Ecosphere, 2018, 9, e02298.	2.2	21

#	Article	IF	CITATIONS
109	Short-term vegetation loss versus decadal degradation of grasslands in the Caucasus based on Cumulative Endmember Fractions. Remote Sensing of Environment, 2020, 248, 111969.	11.0	21
110	Brightness gradient-corrected hyperspectral image mosaics for fractional vegetation cover mapping in northern California. Remote Sensing Letters, 2020, 11, 1-10.	1.4	20
111	Regional matters: On the usefulness of regional landâ€cover datasets in times of global change. Remote Sensing in Ecology and Conservation, 2022, 8, 272-283.	4.3	20
112	Simulation of Multitemporal and Hyperspectral Vegetation Canopy Bidirectional Reflectance Using Detailed Virtual 3-D Canopy Models. IEEE Transactions on Geoscience and Remote Sensing, 2014, 52, 2096-2108.	6.3	19
113	Using Class Probabilities to Map Gradual Transitions in Shrub Vegetation from Simulated EnMAP Data. Remote Sensing, 2015, 7, 10668-10688.	4.0	19
114	Mapping beta diversity from space: Sparse Generalised Dissimilarity Modelling (SGDM) for analysing highâ€dimensional data. Methods in Ecology and Evolution, 2015, 6, 764-771.	5.2	18
115	Global-scale patterns and determinants of cropping frequency in irrigation dam command areas. Global Environmental Change, 2018, 50, 110-122.	7.8	18
116	Impacts of Public and Private Sector Policies on Soybean and Pasture Expansion in Mato Grosso—Brazil from 2001 to 2017. Land, 2020, 9, 20.	2.9	16
117	Operational Coregistration of the Sentinel-2A/B Image Archive Using Multitemporal Landsat Spectral Averages. IEEE Geoscience and Remote Sensing Letters, 2021, 18, 712-716.	3.1	15
118	Applying Imaging Spectrometry in Urban Areas. , 2006, , 137-164.		14
119	Time Series Analyses in a New Era of Optical Satellite Data. Remote Sensing and Digital Image Processing, 2015, , 25-41.	0.7	14
120	Multi-season unmixing of vegetation class fractions across diverse Californian ecoregions using simulated spaceborne imaging spectroscopy data. Remote Sensing of Environment, 2021, 264, 112558.	11.0	14
121	Import Vector Machines for Quantitative Analysis of Hyperspectral Data. IEEE Geoscience and Remote Sensing Letters, 2014, 11, 449-453.	3.1	13
122	Using Landsat to Assess the Relationship Between Spatiotemporal Patterns of Western Spruce Budworm Outbreaks and Regional-Scale Weather Variability. Canadian Journal of Remote Sensing, 2016, 42, 706-718.	2.4	13
123	Beyond deforestation: Differences in long-term regrowth dynamics across land use regimes in southern Amazonia. Remote Sensing of Environment, 2016, 186, 652-662.	11.0	13
124	Synthesizing dam-induced land system change. Ambio, 2019, 48, 1183-1194.	5.5	12
125	A Global MODIS Water Vapor Database for the Operational Atmospheric Correction of Historic and Recent Landsat Imagery. Remote Sensing, 2019, 11, 257.	4.0	11
126	Revisiting the Past: Replicability of a Historic Long-Term Vegetation Dynamics Assessment in the Era of Big Data Analytics. Remote Sensing, 2022, 14, 597.	4.0	11

#	Article	IF	CITATIONS
127	Land Use Competition: Ecological, Economic and Social Perspectives. , 2016, , 1-17.		10
128	Visualizing and labeling dense multi-sensor earth observation time series: The EO Time Series Viewer. Environmental Modelling and Software, 2020, 125, 104631.	4.5	9
129	Landsat time series reveal simultaneous expansion and intensification of irrigated dry season cropping in Southeastern Turkey. Journal of Land Use Science, 2021, 16, 94-110.	2.2	8
130	Long-Term Observation of Mediterranean Ecosystems with Satellite Remote Sensing. , 2005, , 33-43.		7
131	Management Effectiveness and Land Cover Change in Dynamic Cultural Landscapes—Assessing a Central European Biosphere Reserve. Ecology and Society, 2013, 18, .	2.3	7
132	Combining simulated hyperspectral EnMAP and Landsat time series for forest aboveground biomass mapping. International Journal of Applied Earth Observation and Geoinformation, 2021, 98, 102307.	2.8	7
133	Sensing of Photosynthetic Activity of Crops. , 2010, , 87-99.		7
134	Monitoring long-term forest dynamics with scarce data: a multi-date classification implementation in the Ecuadorian Amazon. European Journal of Remote Sensing, 2019, 52, 62-78.	3.5	6
135	Impacts of cutting frequency and position to tree line on herbage accumulation in silvopastoral grassland reveal potential for grassland conservation based on land use and cover information. Annals of Applied Biology, 2021, 179, 75-84.	2.5	6
136	Spatial Epidemiological Applications in Public Health Research: Examples from the Megacity of Dhaka. Contributions To Statistics, 2011, , 243-261.	0.2	6
137	Simplifying Support Vector Machines for Regression analysis of hyperspectral imagery. , 2009, , .		5
138	Analyzing Hyperspectral and Hypertemporal Data by Decoupling Feature Redundancy and Feature Relevance. IEEE Geoscience and Remote Sensing Letters, 2015, 12, 983-987.	3.1	5
139	Advances in Urban Remote Sensing: Examples From Berlin (Germany). , 2007, , 37-51.		5
140	Changes in the grasslands of the Caucasus based on Cumulative Endmember Fractions from the full 1987–2019 Landsat record. Science of Remote Sensing, 2021, 4, 100035.	4.8	5
141	A method to detect and correct single-band missing pixels in Landsat TM and ETM+ data. Computers and Geosciences, 2008, 34, 445-455.	4.2	4
142	Forest Cover Dynamics During Massive Ownership Changes – Annual Disturbance Mapping Using Annual Landsat Time-Series. Remote Sensing and Digital Image Processing, 2015, , 307-322.	0.7	4
143	Mapping woody plant community turnover with spaceâ€borne hyperspectral data – a case study in the Cerrado. Remote Sensing in Ecology and Conservation, 2019, 5, 107-115.	4.3	4
144	Impact of different morphological profiles on the classification accuracy of urban hyperspectral data. , 2009, , .		3

9

#	Article	IF	CITATIONS
145	Using MODIS time series and random forests classification for mapping land use in South-East Asia. , 2012, , .		3
146	Competition for Land-Based Ecosystem Services: Trade-Offs and Synergies. , 2016, , 127-147.		3
147	Historical carbon fluxes in the expanding deforestation frontier of Southern Brazilian Amazonia (1985–2012). Regional Environmental Change, 2018, 18, 77-89.	2.9	3
148	Remote Sensing and Spatial Modelling of the Urban Environment. , 2011, , 231-259.		3
149	Sensitivity study for urban change analysis comparing Landsat-ETM+ and Terra-ASTER data. Proceedings of SPIE, 2004, , .	0.8	2
150	EnMAP-Box 3 a free and open source Python plug-in for QGIS. , 2018, , .		2
151	Sub-pixel building area mapping based on synthetic training data and regression-based unmixing using Sentinel-1 and -2 data. Remote Sensing Letters, 2022, 13, 822-832.	1.4	2
152	Simplifying Support Vector Machines for classification of hyperspectral imagery and selection of relevant features. , 2010, , .		1
153	Comparing Phenometrics Extracted From Dense Landsat-Like Image Time Series for Crop Classification. , 2019, , .		1
154	The Role of Remote Sensing in LTER Projects. , 2010, , 131-142.		1
155	Applying A Phenological Object-Based Image Analysis (Phenobia) for Agricultural Land Classification: A Study Case in the Brazilian Cerrado. , 2020, , .		1
156	Processing Techniques for Hyperspectral Data. Remote Sensing and Digital Image Processing, 2010, , 165-179.	0.7	0